Gravity Wave Interactions with Fine Structures in the Mesosphere and Lower Thermosphere

Email: tyler@gats-inc.com

Tyler Mixa[1,2], Dave Fritts[2], Katrina Bossert[2], Brian Laughman[2], Ling Wang[2], Tom Lund[3], Lakshmi Kantha[1]

[1]University of Colorado Boulder, Boulder, CO, USA
[2]Global Atmospheric Technologies and Sciences (GATS)-inc, Boulder, CO, USA
[3]Northwest Research Associates (NWRA), Boulder, CO, USA

Abstract ID: 11213
OS5.1/AS1.12: Internal Gravity Waves

This presentation participates in OSPP
Outstanding Student Poster & PICO Contest

Significant Findings

- Self-acceleration produces significant departures from modeled and observed behavior of linear gravity wave interactions with stratified layer structures
- In a nonlinear environment, stratified shear structures evolve sharpened vertical gradients and warped orientation as they are advected and enhanced by a passing gravity wave prior to instability onset
- For sufficiently high amplitudes, gravity waves take over influencing instability dynamics – gravity wave vertical wavelength (λ_z) can govern shear instability scales more than initial shear parameters
- In an active wave environment, gravity wave breaking induces background flow deceleration that significantly impacts the interpretation of observational data from ground-based vertical profiling instruments

Introduction

Recent observations identify persistent sheets of high stratification and shear in the MLT. Gravity waves modulate these fine structures to evolve complex instabilities that alter the background flow and change wave propagation and transport properties. Limited observational domains provide an incomplete picture of these dynamics, and most simulation architectures can't characterize the interactions of fine scale structures over a sufficiently large vertical range to discern their influence on wave propagation and transport. Using high resolution simulations of a localized gravity wave packet in a deep atmosphere, we identify the relative impacts of various wave and mean flow parameters to improve our understanding of these dynamics and complement recent state-of-the-art observations.

Observational Motivation

- **KHI chains forming on the upper crest of gravity wave-modulated a shear layers observed in the MLT [e.g. *Lehmacher et al., 2007*; *Pfrommer et al., 2009*; *Baumgarten and Fritts 2014*]**
- **Persistent layer structures < 0.5km deep observed at Alomar, Norway, and Logan, Utah, showing signs of trapped, breaking, and propagating waves**
- **Departures from expected energetic evolution in the MLT imply complex small-scale interactions contributing to localized energy and momentum depositions**

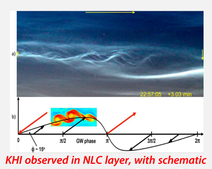

KHI observed in NLC layer, with schematic showing gravity wave influence. Taken from Baumgarten and Fritts 2014.

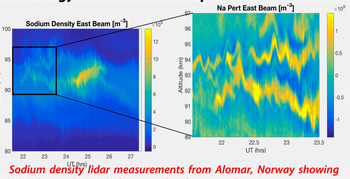

Sodium density lidar measurements from Alomar, Norway showing KHI observed in NLC layer, with schematic showing gravity wave influence. Taken from Bossert et al 2016.

Simulation Architecture

- 3D, anelastic, nonlinear, incompressible finite volume DNS (see *Felten and Lund 2006*)
- Energy-conserving numerical scheme resolves local dissipation scales in the MLT
- Dynamic LES implementation accounts for sub-grid scales, based on the subgrid-scale eddy viscosity model developed by *Germano et al., 1991*
- Captures nonlinear dynamics, including wave contributions to the mean flow evolution
- Non-Boussinesq; density scales with altitude and enables realistic wave amplitude evolution
- Characterize turning layers, unlike ray-tracing routines
- Enables deep atmospheric simulations with sufficient resolution to characterize instabilities through the onset of turbulence

Environmental Parameters

With a fully resolvable inner scale, turbulent influences on dynamics down to σ (1m) are reasonably captured with this model.

altitude	$L_0 = (\epsilon/N^3)^{1/2}$	$L_K = (\nu^3/\epsilon)^{1/4}$
< 3 km	4 m	0.002 m
80-90 km	20-500 m	0.5-2 m

Background Input Fields: $U[z] = U_1 + \frac{U_0 - U_1}{2} + \frac{U_1 - U_0}{2}\tanh\left[\frac{z-z_0}{d}\right]$ $N^2[z] = N_0^2 + (N_1^2 - N_0^2)\ sech^2\left[\frac{z-z_0}{d}\right]$ $T_B = 2\pi/N = 314s$

Resulting Flow Characteristics: $Ri_{min} = \left(\frac{N^2[z_0]}{\left(\frac{dU}{dz}\right)^2[z_0]}\right) = 4N^2\left(\frac{d}{U_1 - U_0}\right)^2$ $T(z < z_0) = 240\ K$ $Re = \frac{(U_1 - U_0)\,d}{2\nu}$ $Re = \frac{\lambda_z^2}{T_B \nu}$

Fine Structure-Induced Instability Evolution

Collocated, Ri-stable Shear and N² Layer

- Initial layers kink and flatten to create deepened region of elevated shear and stability (figures 1, 2)
- Self acceleration stalls vertical packet propagation and triggers wave breaking at 85km near 5 T_B (figure 2)
- Decelerated flow from wave breaking advects packet across domain and detaches w′ phase lines (figure 3)
- Shear reorients w′ perpendicular to u′ and θ′, triggering large KHI dictated by wave λ_z scales (figure 3)
- Secondary KHI form in braid and develop spanwise counter-rotating vortices as turbulence triggered (figure 4)

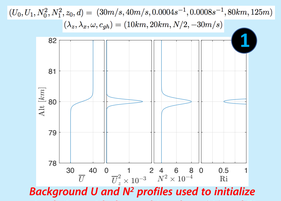

Background U and N² profiles used to initialize simulation, with the resulting shear (U_z) and Ri profiles. The initial Ri is stable, ensuring that all instabilities are caused by interactions with the wave packet.

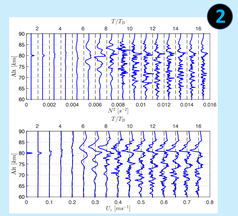

N² and U_z evolution from initial layer structure. Single layers evolve complex stratification when the wave packet propagates through.

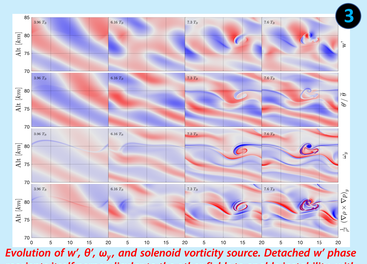

Evolution of w′, θ′, ω_y, and solenoid vorticity source. Detached w′ phase reorients itself perpendicular to the other fields to enable instability, with evidence of strong solenoidal influence on the vortical evolution.

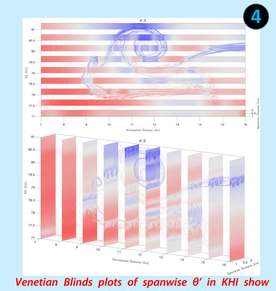

Venetian Blinds plots of spanwise θ′ in KHI show coherent vortex pairs where 3D instability occurs.

Layer Structure Influences

Cases with Shear and N² layer, Shear Layer Only, N² Layer Only, and No Layer

- 3D instability onset hastened by all layer types (figure 1)
- Shear layers promote secondary KE maxima and increase maximum 3D KE (figure 1)
- All layer types produce unique background flow deceleration profiles (figures 2, 3)
- Depth of stratified region extended by wave-layer interaction and apparent modulational instability (figure 3)

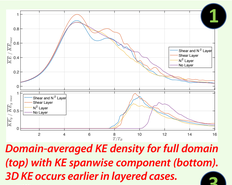

Domain-averaged KE density for full domain (top) with KE spanwise component (bottom). 3D KE occurs earlier in layered cases.

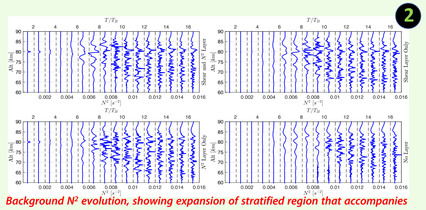

Background N² evolution, showing expansion of stratified region that accompanies apparent modulational instability and turbulence onset.

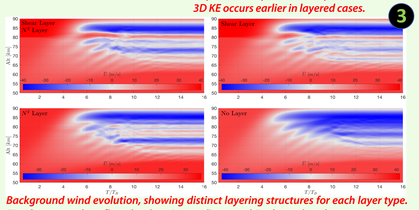

Background wind evolution, showing distinct layering structures for each layer type. Fine layers produce flow deceleration at discrete altitudes rather than a continuous decelerated region.

Wave Amplitude Influences

Cases with Reduced Wave Amplitude Using Initial Shear and N² Layer

- Shear-induced secondary KH maximum only occurs for high amplitude waves (figure 1)
- 3D instability only occurs for high amplitude waves (figure 1)
- Downward extent of flow deceleration lessened by reduced amplitude but still occurs at same altitudes (figure 2)
- Advection of kinked shear layer produces wave-like oscillations in perturbation profiles that are difficult to correctly diagnose with vertical profiling instruments (figure 3)

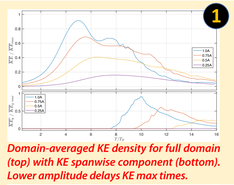

Domain-averaged KE density for full domain (top) with KE spanwise component (bottom). Lower amplitude delays KE max times.

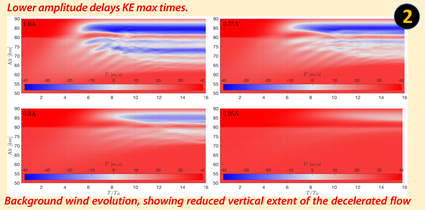

Background wind evolution, showing reduced vertical extent of the decelerated flow region with reduced wave amplitude.

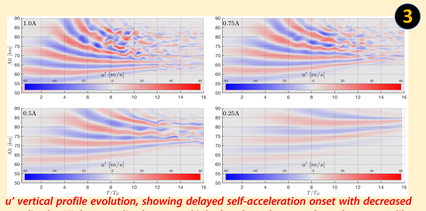

u′ vertical profile evolution, showing delayed self-acceleration onset with decreased amplitude. Higher amplitude waves kink the shear layer and produce wave-like oscillations as decelerated flow advects the layer across the domain.

Wave Propagation Through Lidar-Assimilated Background Profiles

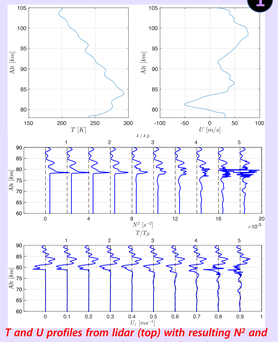

T and U profiles from lidar (top) with resulting N² and shear time evolution. Shear and N² peaks at jet are flattened by the breaking wave, with clear turbulence onset by 4 T_B.

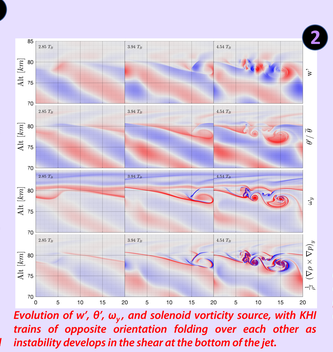

Evolution of w′, θ′, ω_y, and solenoid vorticity source, with KHI trains of opposite orientation folding over each other as instability develops in the shear at the bottom of the jet.

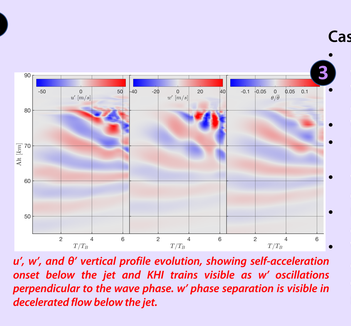

u′, w′, and θ′ vertical profile evolution, showing self-acceleration onset below the jet and KHI trains visible as w′ oscillations perpendicular to the wave phase. w′ phase separation is visible in decelerated flow below the jet.

Case with Alomar Lidar Background Profiles

- Lidar U and T profiles initialized from 80-105km with sharp jet and fine oscillations above (figure 1)
- Wave from initial 1.0A case propagated into complex layered environment (figure 2)
- Wave cutoff at jet and breaks below (figures 2, 3)
- Breaking flattens N² peak and decreases shear below jet while expanding shear region (figure 1)
- w′ phase lines separate at top of packet as local deceleration increases (figures 2, 3)
- Multiple KHI trains develop as layers fold over each other (figure 2)
- Vertical profiles of u′, w′, and θ′ show faster SA onset and separation of w′ phase lines than original 1.0A case with lower shear/N² peaks (figure 3)

Conclusions

Fine layer structures extensively change wave propagation dynamics

- Encourage wave breaking and hasten turbulence onset
- Confine background flow decelerations to discrete altitudes below initial layer
- Instigate modulational instabilities and increase vertical extent of turbulence and stratification effects

Background wind evolution uniquely influenced by layer type and wave amplitude

- *Initial layer type dictates altitude distribution of decelerated background flow regions*
- *Higher amplitude expands the downward propagation envelope of the modulational instability*
- *Lower amplitude deposits energy at the same altitudes within the reduced vertical extent of downward propagation*

Instability and energetics uniquely influenced by layer type and wave amplitude

- *Shear and N² layers both encourage overturning and hasten instability onset*
- *Shear layers increase 3D energy and introduce faster energy drop-off after initial maximum*
- *KE maximum level, times of maximum and falloff, and evolution of 3D instability are dominantly influenced by wave amplitude*

Complexity in interpreting 1D vertical profile measurements

- *Advection of evanescent packet and kinked shear layer mimic the appearance of trapped wave activity in wind perturbations*
- *Relationship between background wind and wave c_{ph} must be considered to accurately identify wave activity where advection speed varies with altitude*

References

Baumgarten, G., & Fritts, D. C. (2014). Quantifying Kelvin-Helmholtz instability dynamics observed in noctilucent clouds: 1. Methods and observations. *Journal of Geophysical Research: Atmospheres*, *119*(15), 9324–9337.

Bossert, K., Fritts, D. C., Yuan, T., Taylor, M. J., & Williams, B. P. (2016). Small-Scale Gravity Wave Propagation and Instability Dynamics in the Presence of Tides. Paper presented at AGU Fall Meeting, December 2016.

Felten, F. N., & Lund, T. S. (2006). Kinetic energy conservation issues associated with the collocated mesh scheme for incompressible flow. *Journal of Computational Physics*, *215*(2), 465–484.

Germano, M., Pomelli, U., Moin, P., & Cabot, W. H. (1991). A dynamic subgrid-scale eddy viscosity model. *Phys. Fluids A Fluid Dyn.*, *3*(7), 1760.

Lehmacher, G. A., Guo, L., Kudeki, E., Reyes, P. M., Akgiray, A., & Chau, J. L. (2007). High-resolution observations of mesospheric layers with the Jicamarca VHF radar. *Advances in Space Research*, *40*(6), 734–743.

Pfrommer, T., Hickson, P., & She, C. Y. (2009). A large aperture sodium fluorescence lidar with very high resolution for mesopause dynamics and adaptive optics studies. *Geophysical Research Letters*, *36*(15), 2–6.